Journal of Computer-Aided Molecular Design, 11 (1997) 71–78
ESCOM

J-CAMD 376

Comparative molecular field analysis and molecular modeling studies of 20-(*S*)-camptothecin analogs as inhibitors of DNA topoisomerase I and anticancer/antitumor agents

Sean W. Carrigan[a], Peter C. Fox[a], Monroe E. Wall[b], Mansukh C. Wani[b] and J. Phillip Bowen[a,*]

[a]*Computational Center for Molecular Structure and Design, Department of Chemistry, University of Georgia, Athens, GA 30602-2556, U.S.A.*
[b]*Research Triangle Institute, Research Triangle Park, NC 27709, U.S.A.*

Received 8 April 1996
Accepted 19 August 1996

Keywords: CoMFA; Camptothecin; MM3

Summary

Conformational studies and comparative molecular field analysis (CoMFA) were undertaken for a series of camptothecin (CPT) analogs to correlate topoisomerase I inhibition with the steric and electrostatic properties of 32 known compounds. The resulting CoMFA models have been used to make predictions on novel CPT derivatives. Using the newly derived MM3 parameters, a molecular database of the 32 CPT analogs was created. Various point atomic charges were generated and assigned to the MM3 minimized structures, which were used in partial least-squares analyses. Overall, CoMFA models with the greatest predictive validity were obtained when both the *R*- and *S*-isomers were included in the data set, and semiempirical charges were calculated for MM3 minimized low-energy lactone structures. A cross-validated R^2 of 0.758 and a non-cross-validated R^2 of 0.916 were obtained for MM3 minimized structures with PM3 ESP charges for the 32 CPT analogs. The derived QSAR equations were used to assign topoisomerase I inhibition values for compounds in this study and compounds not included in the original data set. Prior to its appearance in the literature, an IC_{50} of 103 nM was predicted for the 10,11-oxazole derivative. This CoMFA predicted value compared favorably with the recently reported value of 150 nM. The CoMFA model was also evaluated by predicting the activities of recently reported 11-aza CPT and trione derivatives. The predicted activity (IC_{50} = 249 nM) for 11-aza CPT compared well with the reported value of 383 nM.

Introduction

Since its isolation by Wall and co-workers in 1966 [1], the eukaryotic DNA topoisomerase I inhibitor 20-(*S*)-camptothecin (CPT) (Fig. 1) has been the lead compound for several anticancer drugs currently in clinical trials against a variety of cancers [2,3]. The cytotoxic effects of CPT are a result of the inhibition of eukaryotic DNA topoisomerase I (topo I). Topoisomerases are essential nuclear enzymes which modify the topological state of DNA and are characterized by the number of transient DNA strands breaks produced. Type I topoisomerases act by transient breakage of a single strand of the DNA, allowing the phosphodiester bond on the strand opposite the nick to serve as a swivel point. CPT stabilizes the covalent, reversible topo I–DNA complex leading to inhibition of DNA synthesis in mammalian cells [4] and interferes with the topo I breakage–reunion reaction. CPT reversibly traps the topo I–DNA complex (termed the 'cleavable complex' [5]) in which eukaryotic topo I is covalently linked via a tyrosine residue to a 3'-phosphodiester bond of the DNA [6].

Clinical trials and structure–activity studies have demonstrated the requirement of the α-hydroxy group, the pyridone moiety, and the pentacyclic ring system for maximum activity. The sodium salts of the open form of

*To whom correspondence should be addressed.

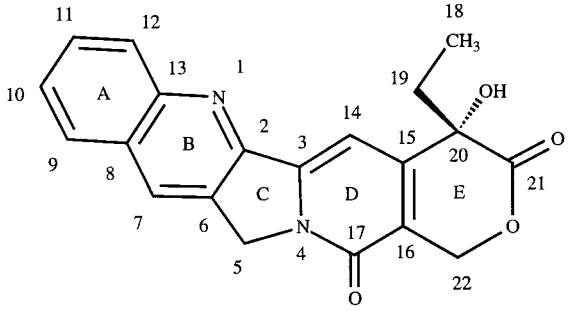

Fig. 1. Structure and numbering system for 20-(*S*)-CPT.

the CPT lactone have much lower activities than the intact lactone itself. It has been suggested that the lactone moiety is required for biological activity, serving as a source for nucleophilic attack at the carbonyl, with subsequent ring opening and covalent bond formation.

The *S*-isomer of CPT is the isomer that exhibits topoisomerase inhibition, while the *R*-isomer has an IC_{50} 1000 times that of its enantiomer. Many CPT derivatives have been synthesized with the goal of enhancing the efficacy and water solubility of these compounds [7–12]. Substitution of the 9 and 10 positions of the A ring by halides and other electron-rich groups (e.g. amino, hydroxy, etc.) generally increases the topo I inhibition of these compounds. The addition of a 10,11-methylenedioxy moiety at the A ring substantially increases the activity, and this functionality is present in several medicinally promising analogs. This has led us to investigate and suggest other heterocyclic analogs fused to the A ring. Substitutions at the 7-position have been found to be more potent, and an increase in water solubility has been observed depending on the nature of the 7-substituent.

Several CPT drug candidates are currently in clinical trials, and new derivatives are being synthesized and reported by a number of groups. The water-soluble hydrochloride salt of 9-dimethylaminomethyl-10-hydroxy camptothecin is in clinical trials under the name topotecan (SmithKline Beecham). 7-Ethyl-10-(4-piperidino)-piperidinylcarbonyloxy camptothecin (also known as CPT 11 or irinotecan) is undergoing clinical trials in Japan for lung, colorectal, cervical, and ovarian cancers [2].

CoMFA

Since its development in the late 1980s, comparative molecular field analysis (CoMFA) [13] has been applied to a wide variety of systems and has shown reasonable predictive performance and versatility unique in computer-based techniques for molecular design [14–16]. The first and crucial step in a CoMFA analysis involves the alignment of molecules in a structurally and pharmacologically reasonable manner, and the overlapped candidates are then stored in a database. A probe atom is placed at all lattice points of a grid or three-dimensional lattice enveloping the entire set of molecular structures. The default probe atom used by CoMFA has the van der Waals properties of an sp^3 hybridized carbon with a unit positive charge. The steric and electrostatic interaction energies between the probe atom and every atom in the molecule are then calculated and stored in a table. Since the resultant tables have many more descriptors than compounds, the statistical method of partial least squares (PLS) [17], a formalism used to analyze data of highly underdetermined character, is used to ensure predictive validity.

Conformational analysis

For an accurate conformational analysis of CPT, the molecular mechanics force field MM3(96) [18] was used. Unfortunately, some of the parameters required to calculate CPT derivatives had not been studied and incorporated into the program. The necessary MM3 torsional

TABLE 1
MM3 STRUCTURES AND RELATIVE ENERGIES OF 20-(*S*)-CPT

Conformation	Final energy (kcal mol^{-1})	Relative energy (kcal mol^{-1})	Ethyl torsion[a] (°)	OH torsion[b] (°)	H···O[c] (Å)	Lactone conformation[d]
1	–2059.4233	0.0000	–57.9	–139.7	2.174	A
2	–2058.9451	0.4772	–179.6	–135.7	2.175	A
3	–2058.6729	0.7504	64.5	–147.9	2.207	A
4	–2052.5044	6.9189	177.9	109.3	3.357	A
5	–2051.4023	8.0210	62.3	40.0	3.396	B
6	–2050.6133	8.8100	–73.3	–163.6	3.025	B
7	–2050.4197	9.0036	–173.5	–153.3	3.060	B
8	–2049.8630	9.5603	–172.5	50.8	4.146	B
9	–2049.3130	10.1103	–72.3	38.3	4.130	B

[a] The ethyl torsion is measured using atoms 15-20-19-18.
[b] The OH torsion is defined using atoms 15-20-O-H.
[c] The H···O distance is the distance between the hydroxyl proton and the lactone carbonyl oxygen.
[d] Lactone conformation type A has the lactone carbonyl on the same side of the CPT plane as the 20-hydroxy group. In the type B conformation, the lactone carbonyl is on the 20-ethyl side of the CPT plane.

parameters were derived prior to undertaking the conformational analysis [19]. Using the newly derived parameters, which are available in MM3(96), a conformational analysis of the α-hydroxy lactone moiety was undertaken. Results with the default dielectric of 1.5 are presented in Table 1.

MM3 conformational studies using a variety of other dielectric constants, ranging from the default value of 1.5 to 80.0, produced similar results. Conformations of 20-(*S*)-CPT in which the lactone carbonyl is on the 20-hydroxy side of the CPT plane are predicted by MM3 to be of lower energy than those in which the lactone carbonyl is on the 20-ethyl side of the CPT plane. These are herein referred to as lactone conformations type A and B, respectively (Figs. 2 and 3).

The MM3 global minimum was found to have a lactone conformation similar to that of the crystal structures of camptothecin iodoacetate [20] and 7-ethyl-10-(4-piperidino)piperidinylcarbonyloxy CPT HCl [21]. Both these X-ray structures have a type A lactone conformation. The most stable MM3 conformations for 20-(*S*)-CPT are the three conformations that show substantial stabilization, and this may be attributed to intramolecular hydrogen bonding as evidenced by the relative energies and smaller hydroxyl proton to carbonyl oxygen distances. As shown in Table 1, *S*-enantiomers in which the carbonyl is on the ethyl side of the CPT plane are several kcal mol^{-1} higher in energy than those in which the carbonyl is on the 20-hydroxy side of the CPT plane. Since the α-hydroxy group is required for activity, the conformational analysis seems to support the hypothesis that intramolecular hydrogen bonding makes the carbonyl more susceptible to nucleophilic attack. Minimizations using the TRIPOS [22] force field matched the results using MM3. One notable difference is that the TRIPOS force field predicted a high-energy, but stable, structure in which the lactone is almost planar but in a twist type conformation. MM3 and semiempirical optimizations did not predict similar twist type conformations. AM1 and PM3 geometry optimizations using SPARTAN 3.1 [23] yielded results similar to MM3 in that the low-energy lactone conformations for the 20-(*S*)-isomers were those which allowed intramolecular hydrogen bonding.

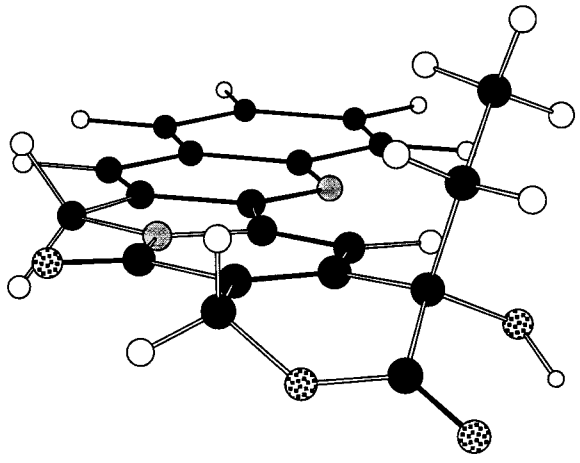

Fig. 2. MM3 low-energy (type A) lactone conformation.

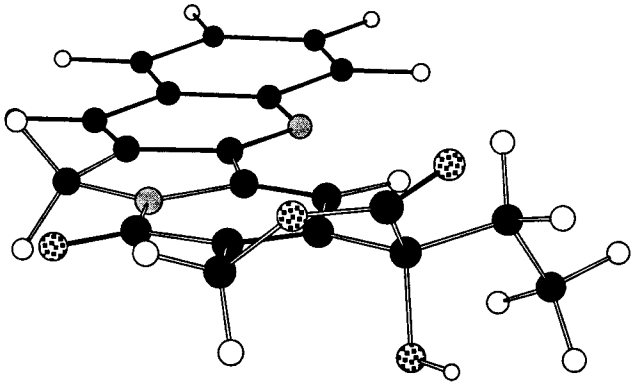

Fig. 3. MM3 high-energy (type B) lactone conformation.

Computational methods

MM3(96) calculations were carried out on IBM RS/6000 and Silicon Graphics workstations. Molecular geometries and CoMFA models were displayed using SYBYL 6.0 running on Silicon Graphics Indigo workstations. The semiempirical calculations were carried out and analyzed using SPARTAN 3.1 on Silicon Graphics workstations.

Results

In recent years, camptothecin analogs have been tested for biological activity using a number of assays. We decided to use 32 camptothecin analogs with previously reported calf thymus topo I IC_{50} data [6] (defined as the concentration that inhibits cleavable complex formation by 50%). The basis for this choice of data was twofold: (i) the assay was in vitro; and (ii) the assay used enantiomerically pure samples. The data are expressed as pIC_{50} for use as the dependent variable (Table 2).

Since many of these CPT analogs are A ring derivatives, it was thought that substituents on ring A might affect the electronic properties of atoms N1 or C7. The analysis of Hammett parameters, however, failed to indicate a correlation with topo I inhibition. Although Hammett parameters for substituted quinolines also failed to yield a correlation with topoisomerase inhibition, the basicity of the quinoline type nitrogen was investigated using computational models. The SPARC [24] program, which is used to calculate the pK_a of an acid, predicted a pK_a of 4.6 for the nitrogen of quinoline, which compares reasonably well with the reported values of 4.90 [25] and 4.85 [26]. For CPT, however, SPARC predicted a quinoline pK_a of 2.4 versus the experimentally observed value of 1.18 [27]. The pK_a's of substituted quinolines were

calculated using the SPARC program, but no absolute correlation between the calculated pK_a of the quinoline nitrogen and topo I inhibition of the analogously substituted CPT derivatives was found.

To see if any correlation existed between in vitro topo I inhibition and point atomic charges on the atoms of rings A and B, semiempirical AM1 and PM3 geometry optimizations were carried out with SPARTAN 3.1. Point atomic charges were analyzed for all atoms in rings A and B. Plots of semiempirical atomic charges versus pIC_{50} showed a possible correlation between increased positive charge on C7 and increased topoisomerase inhibition. The more rigorous ab initio methods were applied to comparably substituted quinolines. Ab initio geometry optimizations utilizing the RHF/6-31G** basis set on substituted quinolines did not show appreciable changes in point atomic charges. Charges obtained using semiempirical geometry optimizations of the substituted camptothecins had significantly broader ranges than corresponding ab initio calculations. Although the Mulliken semiempirical charges changed little for all the 32 compounds, the semiempirical ESP charges showed more variation. AM1 ESP charges on C7 ranged from less than zero to approximately +0.3, and there was a fairly constant value of –0.6 on N1. The PM3 ESP charges on C7 ranged from about +0.1 to +0.4, while the N1 charges remained fairly constant at about –0.6. However, ab initio calculations on comparably substituted quinolines did not appreciably change the atomic charge on the quinoline type nitrogen or the carbon opposite the nitrogen. The ab initio Mulliken charges were essentially constant at about –0.58 for the nitrogen and close to neutral for C7. The ab initio ESP charges on the comparably substituted quinolines were fairly constant at about –0.7 for N1, and about 0 to +0.15 for C7. In effect, for comparably substituted quinolines, the atomic charges on atoms N1 and C7 showed very little change for a variety of substituents (chloro, hydroxy, amino, fluoro, nitro, methyl, and cyano).

TABLE 2
DNA TOPOISOMERASE I INHIBITION DATA OF CPT ANALOGS USED IN THIS STUDY

Compound	IC_{50} (μM)	SE[a] of IC_{50}	pIC_{50}	CoMFA[b] pIC_{50}
1 20-(*S*)-10,11-MDO[c]	0.027	0.005	1.5686	1.282
2 20-(*S*)-9-Me	0.038	0.013	1.4202	0.797
3 20-(*S*)-9-NH_2-10,11-MDO	0.048	0.016	1.3187	1.472
4 20-(*S*)-9-Cl-10,11-MDO	0.061	0.019	1.2146	1.480
5 20-(*S*)-9-Cl	0.086	0.054	1.0655	0.805
6 20-(*S*)-10-OH	0.106	0.031	0.9747	0.747
7 20-(*S*)-9,10-dichloro	0.108	0.029	0.9666	0.833
8 20-(*S*)-9-NH_2	0.111	0.024	0.9547	0.881
9 20-(*S*)-10-Br	0.126	0.040	0.8996	0.387
10 20-(*S*)-10-NH_2	0.140	0.022	0.8539	0.729
11 20-(*S*)-10-Cl	0.141	0.027	0.8508	0.547
12 20-(*S*)-9-NO_2-10,11-MDO	0.150	0.043	0.8239	1.095
13 20-(*S*)-9-F	0.163	0.074	0.7878	0.683
14 20-(*S*)-10-Me	0.295	0.080	0.5302	0.641
15 20-(*S*)-10-F	0.368	0.194	0.4342	0.555
16 20-(*S*)-10-NO_2	0.635	0.116	0.1972	0.166
17 20-(*S*)-camptothecin	0.677	0.215	0.1694	0.603
18 20-(*S*)-10,11-MDO Na^+ salt	0.843	0.681	0.0742	–0.292
19 20-(*S*)-9-OH	0.873	0.302	0.0590	0.712
20 20-(*S*)-10-carboxy	1.022	0.319	–0.0095	–0.022
21 20-(*S*)-9-DMAM[d]-10-OH	1.046	0.438	–0.0195	0.123
22 20-(*S*)-9-DMAM-10-OH HCl	1.110	NA	–0.0453	0.022
23 20-(*S*)-10-CN	1.939	0.362	–0.2876	0.156
24 20-(*S*)-10-OH di Na^+ salt	3.202	0.603	–0.5054	–0.399
25 20-(*S*)-9-NH_2-10,11-MDO Na^+	4.303	2.512	–0.6338	–0.412
26 20-(*S*)-10-(4-Mepiperazino)carbonyloxy	4.401	6.484	–0.6436	–0.601
27 20-(*S*)-CPT Na^+ salt	11.586	5.852	–1.0639	–0.901
28 20-(*S*)-10-(dipiperidinyl)carbonyloxy	20.546	18.551	–1.3127	–1.325
29 20-(*R*)-10,11-MDO Na^+ salt	> 30		–1.477	–1.626
30 20-(*R*)-9-NH_2-10,11-MDO	> 30		–1.477	–1.294
31 20-(*R*)-10,11-MDO	> 30		–1.477	–1.464
32 20-(*R*)-CPT	> 30		–1.477	–1.467

[a] SE: standard error.
[b] Predicted values from the final CoMFA model ($R^2 = 0.916$).
[c] MDO: methylenedioxy.
[d] DMAM: dimethylaminomethyl.

TABLE 3
CoMFA ANALYSES USING MM3 LOW-ENERGY CONFORMATIONS OF CPT ANALOGS (DEL RE CHARGES APPLIED AFTER MINIMIZATION) SHOWING INFLUENCE OF SUBGROUP CHOICE

Cross-validation groups	Compounds	Maximum number of components tested (optimum)	Cross-validated R^2 (SE)	Non-cross-validated R^2 (SE)
5	32 (all)	5 (4)	0.667 (0.585)	0.868 (0.368)
5	28 (only *S*)	5 (3)	0.540	
5	27 (no salts)	5 (4)	0.666	
5	24 (no salts, no *R*)	5 (2)	0.466	
32	32 (all)	5 (4)	0.727 (0.530)	0.868 (0.368)

Molecular databases containing the 32 camptothecin analogs were generated using both the TRIPOS and MM3 force fields. Using the MM3 minimized structures, CoMFA gave better predictive models than those derived from the TRIPOS force field. All 20-(*S*)-enantiomers in the CoMFA databases had identical lactone conformations. For our 3D QSAR studies using the MM3 low-energy (type A) lactone conformations, the *S*-isomers were in the lowest energy (type A) conformation, and the *R*-isomers were also in their (mirror image) low-energy lactone conformation.

Due to the rigidity of the CPT skeleton, the task of molecular alignment was greatly simplified. After some trial and error, an rms fit using atoms 2, 3, and 6 of the central five-membered ring was selected to define the alignment. The default lattice spacing of 2.0 Å was found to yield the best results. The default probe atom was found to give good results for our system. Changing the probe atom to an oxygen with a −1.0 charge (or a carbon with a −1.0 charge) resulted in a decrease in the predictive value of the model.

For the PLS statistics, the optimum number of components, or the level of model complexity, was determined first [28]. Once the optimum number of components was determined, the non-cross-validated PLS analyses produced a non-cross-validated QSAR equation with an R^2 between 0.0 and 1.0. Gasteiger–Hückel, Del Re, Pullman, AM1 and PM3 charges were calculated for the MM3 optimized structures. Next, the runs were saved and the PLS statistics were analyzed (i.e. the actual versus calculated and residual values). The resultant 3D QSAR model has been used to predict the activity of new compounds not included in the original data set.

Various subgroups of the original data set were selected and run in CoMFA. As shown in Table 3, the best results were obtained when all 32 compounds were included in the analysis. Omission of the *R*-isomers, the carboxylate salts, or both, failed to improve the R^2 of the analysis. The analyses in Table 3 used the MM3 lowest energy structures with Del Re (SYBYL) calculated charges.

CoMFA was carried out using both the low-energy (type A) lactones and the higher energy (type B) lactones. As shown in Tables 4 and 5, better results were observed using the MM3 low-energy structures, which gave better cross-validated R^2 values and lower standard errors. Also, a lower optimum number of components, which is desirable, was found when the type A conformations were used.

Log P values for the 32 CPT analogs were calculated using the Moriguchi model [29] (Table 6). Differences in molecular volume and the calculated log P values, when added to CoMFA tables however, failed to improve the CoMFA model.

TABLE 4
EFFECT OF ATOMIC CHARGES ON QSAR ANALYSIS OF MM3 LOW-ENERGY (TYPE A) STRUCTURES (LEAVE-ONE-OUT = 32 CROSS-VALIDATED GROUPS)

Charges applied to MM3 structure	Cross-validated R^2 (SE)	Optimum number of components	Non-cross-validated R^2 (SE)
Gasteiger–Marsili	0.735 (0.522)	4	0.874 (0.360)
Hückel	0.768 (0.488)	4	0.892 (0.333)
Gasteiger–Hückel	0.747 (0.501)	3	0.865 (0.366)
Del Re	0.727 (0.530)	4	0.868 (0.368)
Pullman	0.746 (0.511)	4	0.890 (0.337)
AM1 (Mulliken)	0.723 (0.533)	4	0.883 (0.347)
AM1 (ESP)	0.738 (0.539)	6	0.912 (0.313)
PM3 (Mulliken)	0.748 (0.529)	6	0.923 (0.292)
PM3 (ESP)	0.758 (0.519)	6	0.916[a] (0.306)

[a] Final CoMFA model used for predictions. CoMFA box low corner X = −9.622, Y = −10.239, Z = −10.631, high corner X = 18.815, Y = 8.800, Z = 7.637. Stepsize = 2.00 Å. Final model based on stepwise cross-validated R^2 values of (1) 0.152, (2) 0.574, (3) 0.695, (4) 0.731, (5) 0.746, and (6) 0.758.

TABLE 5
EFFECT OF ATOMIC CHARGES ON QSAR ANALYSIS OF MM3 HIGH-ENERGY (TYPE B) STRUCTURES (LEAVE-ONE-OUT = 32 CROSS-VALIDATED GROUPS)

Charges applied to MM3 structure	Cross-validated R^2 (SE)	Optimum number of components	Non-cross-validated R^2 (SE)
Gasteiger–Marsili	0.724 (0.565)	7	0.934 (0.275)
Hückel	0.764 (0.502)	5	0.896 (0.334)
Gasteiger–Hückel	0.761 (0.505)	5	0.898 (0.330)
Del Re	0.711 (0.556)	5	0.891 (0.342)
Pullman	0.751 (0.516)	5	0.896 (0.333)
AM1 (ESP)	0.738 (0.529)	5	0.900 (0.327)
PM3 (ESP)	0.747 (0.541)	7	0.931 (0.282)

TABLE 6
CALCULATED MORIGUCHI log P VALUES FOR CPT ANALOGS USED IN THIS STUDY

Compound	Calculated log P
1 20-(*S*)-10,11-MDO	1.54309
2 20-(*S*)-9-Me	2.64455
3 20-(*S*)-9-NH_2-10,11-MDO	0.804083
4 20-(*S*)-9-Cl-10,11-MDO	1.76187
5 20-(*S*)-9-Cl	2.64455
6 20-(*S*)-10-OH	1.66243
7 20-(*S*)-9,10-dichloro	2.86334
8 20-(*S*)-9-NH_2	1.66243
9 20-(*S*)-10-Br	2.75446
10 20-(*S*)-10-NH_2	1.66243
11 20-(*S*)-10-Cl	2.64455
12 20-(*S*)-9-NO_2-10,11-MDO	1.44771
13 20-(*S*)-9-F	2.5336
14 20-(*S*)-10-Me	2.64455
15 20-(*S*)-10-F	2.5336
16 20-(*S*)-10-NO_2	2.2731
17 20-(*S*)-camptothecin	2.42157
18 20-(*S*)-10,11-MDO Na^+ salt	–0.00792
19 20-(*S*)-9-OH	1.66243
20 20-(*S*)-10-CO_2	1.06313
21 20-(*S*)-9-DMAM-10-OH	1.57072
22 20-(*S*)-9-DMAM-10-OH HCl	1.57072
23 20-(*S*)-10-CN	1.81146
24 20-(*S*)-10-OH di Na^+ salt	0.1021
25 20-(*S*)-9-NH_2-10,11-MDO Na^+	–0.738744
26 20-(*S*)-10-(4-Mepiperazino)carbonyloxy	2.27407
27 20-(*S*)-camptothecin Na^+ salt	0.850428
28 20-(*S*)-10-(4-dipiperidino)carbonyloxy	3.25201
29 20-(*R*)-10,11-MDO Na^+ salt	–0.00792
30 20-(*R*)-9-NH_2-10,11-MDO	0.804083
31 20-(*R*)-10,11-MDO	1.54309
32 20-(*R*)-camptothecin	2.42157

TABLE 7
PREDICTED AND ACTUAL VALUES FOR 11-AZA ANALOGS

Compound	CoMFA predicted IC_{50} (nM)	Actual IC_{50} [a] (nM)
11-aza CPT	249	383
11-aza-*N*-Me CPT	273	1461
11-aza-*N*-oxide CPT	243	1184

[a] Data taken from Ref. 28, Table 1.

Figure 4 shows the actual and predicted pIC_{50} for the non-cross-validated CoMFA model using the MM3 minimized low-energy structures with PM3 charges applied using the optimum number of components (six). The corresponding R^2 for this analysis was 0.916.

Using this CoMFA model, predictions of biological activity for new analogs have been carried out. After synthesis and evaluation, the actual and predicted topo I activities may be compared. It appears the CoMFA model is useful for compounds having substituents on the A ring since the majority of compounds in this study were A ring derivatives. Indeed, the CoMFA model using the MM3 low-energy conformations, with PM3 applied charges, was used to predict the activity of a number of previously unreported CPT derivatives, where a five-membered heterocycle is fused onto the 10 and 11 positions of ring A.

Prior to any laboratory synthesis, we carried out extensive molecular modeling studies on 10,11-substituted aromatic heterocycles. One promising candidate was the 10,11-oxazole analog (Fig. 5). An IC_{50} of 103 nM was calculated for this 10,11-oxazole derivative. This com-

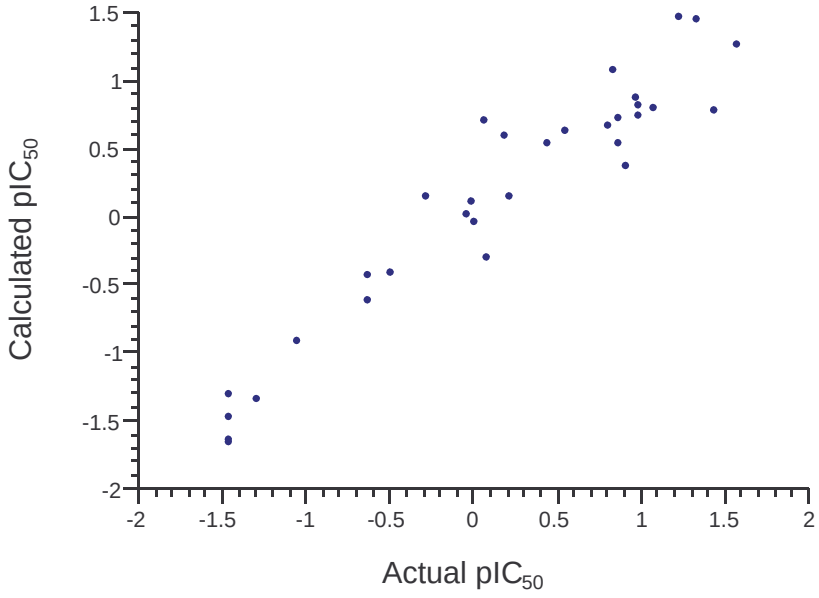

Fig. 4. Actual and predicted pIC_{50} values for the 32 CPT analogs used in this study. Non-cross-validated ($R^2 = 0.916$) CoMFA analysis using MM3 low-energy structures with PM3 charges.

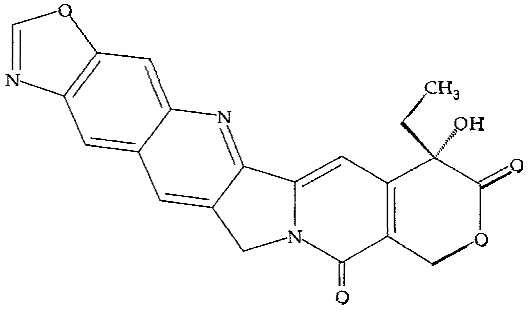

Fig. 5. 10,11-Oxazole CPT.

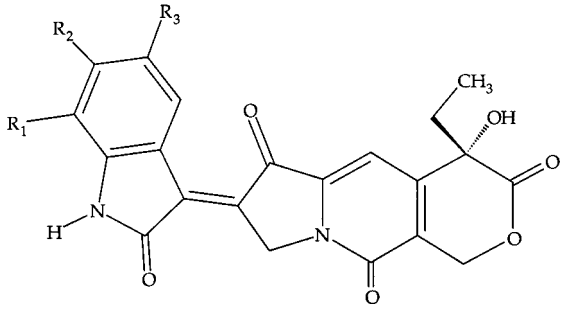

Fig. 6. Recently reported CPT-like trione compounds. R_1, R_2, and R_3 are listed in Table 8.

pound was subsequently synthesized by Glaxo scientists and gave an IC_{50} of 150 nM [30].

In addition to testing the CoMFA model on novel, previously unreported compounds such as the 10,11-oxazole derivative, we have also tested our model on compounds taken directly from the literature but not used in the original data set, such as 11-aza CPT. While 12-aza CPT is less active and less potent than CPT in P-388 leukemia, the 10-aza CPT exhibits modest activity in L-1210 at low doses [8]. 11-aza CPT was recently reported to have approximately twice the activity of CPT [31]. The predicted and experimental values for the 11-aza derivatives are reported in Table 7.

The predicted IC_{50} value of 249 nM for 11-aza CPT compares reasonably well with the reported value of 383 nM. (For reference, CPT has an IC_{50} of 677 nM.) In contrast, the N-methylated 11-aza CPT and the 11-aza-*N*-oxide CPT derivatives were predicted to be on the same order of activity but were less active than CPT in topo I inhibition.

Another set of CPT-like compounds whose pentacyclic ring structure was replaced with a different rigid skeletal framework has recently been reported (Fig. 6) [32]. Topo I inhibition values were predicted for these derivatives.

These compounds have been identified as 8(*RS*)-ethyl-2-(2-oxo-1,2-dihydroindol-3-ylidene)-8-hydroxy-2,3,5,8-tetrahydro-6-oxa-3a-azacyclopenta[*b*]naphthalene-1,4,7-triones. Topo I inhibition values were predicted for these derivatives, and the comparison between the predicted and actual pIC_{50} values (enantiopure samples) is presented in Table 8. MM3 minimized planar conformations for these triones were used for the analysis. For the alignment, the five-membered ring of the trione that is adjacent to the pyridone ring was superimposed onto the five-membered ring of the camptothecin analogs.

TABLE 8
PREDICTED VERSUS ACTUAL IC_{50} VALUES FOR TRIONE DERIVATIVES IN FIG. 6

R_1	R_2	R_3	IC_{50} (actual)[a] (μM)	IC_{50} (pred.) (μM)
H	H	F	1.1	0.131
H	F	F	1.3	0.227
H	H	Me	1.8	0.121
H	H	H	4.0	0.180
H	H	I	12.1	0.128
H	H	Br	>100	0.121
Cl	H	H	>100	0.188
Me	H	H	>100	0.190
NO_2	H	Me	>100	0.328
H	CF_3O	H	>100	0.426

[a] Ref. 29, Table 1.

Discussion

Since the majority of CPT derivatives in this study were A ring substituted, the resulting CoMFA models are of greatest use for other A ring analogs, such as the 10,11-oxazole or the 11-aza CPT. Although the CoMFA model does not predict the topo I inhibition of the triones in Fig. 6 with great accuracy, it does illustrate the qualitative value of the CoMFA model. Four of the five compounds with the highest predicted topo I inhibition were also in the top half of actual topo I inhibition. These results further support the qualitative usefulness of this model.

Other CPT derivatives did not produce successful CoMFA correlations. The 9,10-substituted 9-aminoalkyl derivatives reported by a group at SmithKline Beecham resulted in the development of 9-[(dimethylamino)methyl]-10-hydroxy CPT for clinical use [9]. Our CoMFA model using these compounds produced less satisfactory models. This may in part be attributed to the considerable conformational flexibility in some of these derivatives.

Conclusions

Using the recently derived MM3 parameters, the conformational analysis of CPT indicates that the low-energy CPT conformations are stabilized by intramolecular hydrogen bonding in the gas phase. The low-energy (type A) conformation matches the two reported X-ray structures. Geometry optimizations using AM1 and PM3 are in agreement with MM3. Minimizations using the TRIPOS force field, however, predict a stable, almost planar, but somewhat twisted lactone conformation.

CoMFA models with the greatest predictive value were obtained when the inactive carboxylates, and four of the much less active *R*-isomers, were included in the analyses. Interestingly, topo I inhibition values for compounds such as 10,11-oxazole CPT (Fig. 5) were predicted prior to their laboratory synthesis, and the predicted value of 103 nM compares well with the reported value of 150 nM. Other compounds reported in the literature but not used in the development of the CoMFA model, such as the 11-aza analog and the trione derivatives in Fig. 6, were subjected to CoMFA with favorable results. Overall, this approach to molecular design has yielded promising comparisons between theory and experiment.

Acknowledgements

The authors would like to thank IBM, Silicon Graphics, Tripos Associates, and Wavefunction Inc. for hardware and software grants. We would also like to thank the Georgia Research Alliance and Tripos Associates for their support of the Computational Center for Molecular Structure and Design at the University of Georgia.

References

1 Wall, M.E., Wani, M.C., Cook, C.E., Palmer, K.H., McPhail, A.T. and Sim, G.A., J. Am. Chem. Soc., 88 (1966) 3888.
2 Tanizawa, A., Fujimoro, A., Fujimoro, Y. and Pommier, Y., J. Natl. Cancer Inst., 86 (1994) 836.
3 Verweij, J., Eur. J. Cancer, 31A (1995) 828.
4 Hsiang, Y.W., Liu, L.F., Wall, M.E., Wani, M.C., Nicholas, A.W., Manikumar, G., Kirschenbaum, S., Silber, R. and Potmesil, M., Cancer Res., 49 (1989) 4385.
5 Hsiang, Y.W., Lihou, M.G. and Liu, L.F., Cancer Res., 49 (1989) 5077.
6 Champoux, J., J. Biol. Chem., 256 (1981) 4805.
7 Wall, M.E., Wani, M.C., Nicholas, A.W., Manikumar, G., Tele, C., Moore, L., Truesdale, A., Leitner, P. and Besterman, J.M., J. Med. Chem., 36 (1993) 2689.
8 Wani, M.C., Nicholas, A.W. and Wall, M.E., J. Med. Chem., 29 (1986) 2358.
9 Kingsbury, W.D., Boehm, J.C., Jakas, D.R., Holden, K.G., Hecht, S.M., Gallagher, G., Caranfa, M.J., McCabe, L.F., Johnson, R.K. and Hertzberg, R.P., J. Med. Chem., 34 (1991) 98.
10 Ejima, A., Terasawa, H., Sugimori, M., Ohsuki, S., Matsumoto, K., Kawato, Y., Yasuoka, M. and Tagawa, H., Chem. Pharm. Bull., 40 (1992) 683.
11 Sawada, S., Matsuoka, S., Nokata, K., Nagata, H., Furuta, T., Yokokura, T. and Miyasaka, T., Chem. Pharm. Bull., 93 (1991) 3183.
12 Sawada, S., Nokata, K., Furuta, T., Yokokura, T. and Miyasaka, T., Chem. Pharm. Bull., 39 (1991) 2574.
13 Cramer, R.D., Patterson, D.E. and Bunce, J.D., J. Am. Chem. Soc., 110 (1988) 5959.
14 Carroll, F.I., Gao, Y., Rahman, A.R., Abraham, P., Parham, K., Lewin, A., Boja, J.W. and Kuhar, M.J., J. Med. Chem., 34 (1991) 271.
15 Diana, G.D., Kowalczyk, P., Treasurywala, A.M., Oglesby, R.C., Pevear, D.C. and Dutko, F.J., J. Med. Chem., 35 (1992) 1002.
16 McFarland, J.W., J. Med. Chem., 35 (1992) 2543.
17 Stahle, S. and Wold, S., In Ellis, G.P. and West, G.B. (Eds.) Progress in Medicinal Chemistry, Elsevier, Amsterdam, The Netherlands, 1988, pp. 292–338.
18 Allinger, N.L., Yuh, Y.H. and Lii, J.H., J. Am. Chem. Soc., 111 (1989) 8551.
19 Carrigan, S.W., Lii, J.-H. and Bowen, J.P., J. Comput.-Aided Mol. Design, 11 (1997) 61.
20 McPhail, A.T. and Sim, G.A., J. Chem. Soc., B (1968) 923.
21 Sawada, S., Okajima, S., Aiyama, R., Nokata, K., Furuta, T., Yokokura, T., Sugino, E., Yamaguchi, K. and Miyasaka, T., Chem. Pharm. Bull., 39 (1991) 1441.
22 SYBYL 6.0, Tripos Associates Inc., St. Louis, MO, U.S.A., 1993.
23 SPARTAN 3.1, Wavefunction Inc., Irvine, CA, U.S.A., 1994.
24 Hilal, S.H. and Karickoff, S.W., Quant. Struct.–Act. Relatsh., 14 (1995) 348.
25 Lide, D.R. (Ed.) Handbook of Chemistry and Physics, 74th ed., CRC, Cleveland, OH, U.S.A., 1994.
26 Jencks, W.P. and Regenstein, J., In Fasman, G.D. (Ed.) Handbook of Biochemistry and Molecular Biology, 3rd ed., Physical and Chemical Data, Vol. 1, CRC, Cleveland, OH, U.S.A., 1976, pp. 310–342.
27 Fassberg, J. and Stella, V.J., J. Pharm. Sci., 81 (1992) 676.
28 Suggestions from SYBYL manual, SYBYL 6.0, Tripos Inc., St. Louis, MO, U.S.A., 1992.
29 Moriguchi, I., Hirono, S., Liu, Q., Nakagome, I. and Matsushita, Y., Chem. Pharm. Bull., 40 (1992) 127.
30 Peel, M.R., Milstead, M.W., Sternbach, D.D., Besterman, J.M., Leitner, P., Morton, B. and Wall, M.E., Bioorg. Med. Chem. Lett., 5 (1995) 2129.
31 Uehling, D.E., Nanthakumar, S.S., Croom, D., Emerson, D.L., Leitner, P.P., Luzzio, M.J., McIntyre, G., Morton, B., Profeta, S., Sisco, J., Sternbach, D.D., Tong, W.Q., Vuong, A. and Besterman, J.M., J. Med. Chem., 38 (1995) 1106.
32 Lackey, K., Besterman, J.M., Fletcher, W., Leitner, P., Morton, B. and Sternbach, D.D., J. Med. Chem., 38 (1995) 906.